Surface Analysis of Bacterial Cellulose Membrane Made from Biowaste Added with ZnO Nanopowder

Naufal Rizky Amasda[1], Heru Suryanto[2*], Uun Yanuhar[3], Aminnudin[2], Fajar Nusantara[1], Quota Alief Sias[4]

[1]*Department of Mechanical and Industrial Engineering, Faculty of Engineering, State University of Malang, Jl. Semarang 5, Malang 65145, Indonesia*
[2]*Centre Excellent for Cellulose Composite (CECCom), Department of Mechanical and Industrial Engineering, Universitas Negeri Malang, Malang, East Java, Indonesia*
[3]*Department of Aquatic Resources Management, FPIK, Brawijaya University, East Java, Indonesia*
[4]*Electrical Engineering Department, Chonnam National University, Gwangju, South Korea*
**Corresponding author: heru.suryanto.ft@um.ac.id*

Article history:
Received: 24 December 2024 / Received in revised form: 7 July 2025 / Accepted: 11 July 2025
Available online 20 July 2025

ABSTRACT

Utilization of pineapple biowaste is important to increase the value added to biowaste and solve the environmental problem. So, the study objective is to synthesize membranes of bacterial cellulose made from pineapple biowaste and characterize the surface morphology and porosity of the membrane after being added with ZnO nanopowder. The study starts with extracting biowaste as a bacterial cellulose culture medium for the fermentation process. The obtained pellicle was crushed and homogenized with the added ZnO nanopowder in the presence of ultrasonic waves. The membrane is dried in the oven. The membrane morphology was monitored using scanning electron microscope and Brunauer–Emmett–Teller analysis. Results indicate that surface morphology more rougher in line with increasing ZnO nanopowder content. The control membrane exhibits the highest surface area (36.9605 m^2/g) due to its uninterrupted porous network. The addition of ZnO nanopowder at 2.5% significantly reduces the surface area to 2.9168 m^2/g, likely due to nanoparticle-induced pore obstruction. As the ZnO nanopowder concentration increases to 5% and 7.5%, the specific surface area rises to 8.0436 m^2/g and 13.7783 m^2/g, respectively. This trend suggests that higher ZnO nanopowder loading enhances porosity and introduces additional adsorption sites. The control BC membrane exhibits the highest pore volume and well-defined mesoporosity, which are diminished upon the initial addition of ZnO nanopowder.

Keywords: *Bacterial cellulose, biowaste, Brunauer–Emmett–Teller, porosity, surface morphology, ZnO.*

I. Introduction

Pineapple (*Ananas comosus*) is a significant agricultural commodity. In 2023, Indonesia's pineapple production reached approximately 3.156 billion tons, with forecasts predicting an increase to 3.36 billion tons by 2027 [1][2]. Improper handling of fruits can cause substantial damage, resulting in the loss of up to 55% of the produce and generating significant waste. The increasing production of processed pineapple products also leads to the generation of large amounts of waste annually. Effectively managing pineapple biowaste is a challenge for environmental issues [3]. Eco-friendly approaches to utilizing pineapple biowaste are crucial for adding value. Bioconversion is a powerful method for transforming biomass into phytochemicals, antioxidants, and biofuels [4]. An alternative conversion

DOI: 10.17977/um016v9i12025p281

method is utilizing pineapple biowaste to form a bacterial cellulose product [5] that can reduce environmental harm [6] and offer significant advantages.

The bacteria cellulose producer can synthesize (1–4)-β-D-glucose units, forming ribbon-shaped biopolymers with three-dimensional networks known as bacterial cellulose (BC) or pellicle [7]. Pure BC has interesting structural characteristics that make it a suitable biomaterial matrix for composite membranes. Some researchers utilize BC to form membranes for various applications, including catalysts [8], fuel cells [9], wound dressings [10], and membrane filters [11]. Adding nanoparticles into composite BC membranes improves their potential impact and capabilities. These composites improve the limitations of pure BC and enhance its performance. Some nanopowder has been added as reinforcement, such as carbon nanotubes [12], titanium dioxide and graphene oxide [13], to BC membranes to improve their characteristics. Another type of nanomaterial, zinc oxide (ZnO) nanopowder, is an interesting material for membrane reinforcement due to being available cheaply and abundantly [14]. Besides their unique characteristics, including electrical, structural, and optical [15] and also antimicrobial activity [16].

Zinc oxide nanoparticles are distinguished as a viable alternative due to their compatibility with biological systems and efficacy against various bacterial strains [17],[18]. Simultaneously, due to the increasing demand for sustainable materials, bacterial cellulose has garnered interest as a viable matrix for nanocomposites [19]. Nevertheless, although ZnO nanoparticles are widely recognized for their antibacterial efficacy, achieving uniform dispersion and stable integration within biopolymeric matrices like bacterial cellulose (BC) remains difficult [20]. Furthermore, there is still a lack of studies on the combined effects of ZnO incorporation into bacterial cellulose (BC) membranes, especially with regard to comprehending its influence on the structural stability and general functionality of the membrane [21],[22]. These research gaps underscore the importance of further investigation to refine the integration process and assess the viability of the resulting composite material for advanced membrane technologies.

The use of pineapple biowaste not only overcomes the issue of solid biowaste management in the city to successful in goal of SDGs 11. The expenses required to address these impacts significantly surpass the costs of developing and sustaining efficient biowaste management systems [23]. By using pineapple biowaste as a precursor to synthesize BC-based composite membranes with ZnO nanopowder reinforcement, this study aims to analyze the surface morphology and porosity of BC after adding with ZnO nanopowder using scanning electron microscope and Brunauer–Emmett–Teller analysis so contributing to valorize of agricultural biowaste for sustainable environment.

II. Materials and Methods

1. Materials

The biowaste is sourced from pineapple obtained from the fruit market in Malang, Indonesia. *Acetobacter xylinum,* as a fermentation bacterium, was obtained from the Microbiology Lab., UMM, Malang, Indonesia. ZnO nanopowder was purchased from Hongwu Materials, China, with particle sizes of 20-30 nm. Chemical materials include ammonia acid (Loba-Chemie, India), acetic acid (Smart-Lab. India), urea (Kanto-Chemical, Japan), glucose (Lansida, Indonesia), and sodium hydroxide (Loba-Chemie, India).

2. Synthesis of Bacterial Cellulose

The procedure of synthesis of BC is described in a previous study [18]. The medium for fermentation contained mixing of 5.0 g of ammonium acid and 100.0 g of glucose in 1.0 L of pineapple biowaste extract. Acetic acid was dropped to set the pH at 4.5. To initiate fermentation, *A. xylinum* was added at a volume of 100 mL, and fermentation was conducted under static conditions at 25–30°C. After ten days, the BC at the floated surface medium was harvested and washed with dH_2O until the pH reached 7.0.

3. Production of Membrane

BC membranes production was conducted following Sarjono *et al*. methods [24]. BC pellicles were chopped into small pieces, then pretreated with NaOH solution with a concentration of 6% and boiled at 90°C for 2 hours, then rinsed. Prepared BC pellicles of 300g were soaked in 250 ml distilled water and crushed using a blender (Fomac, China) 3 times for 10 min at 25,000 rpm. The resulting BC colloid was diluted by 0.750L distilled water and then defibrilated in a mechanically homogenizer (AH-100D type, Berkley-Scientific, China) for 5 cycles at 150.0 bar for each cycle. Homogenized BC colloid was filtered, and BC slurry was used for the membrane matrix.

4. Synthesis of Composite Membrane

ZnO nanopowder was grouped in the content of 2.5% (2.5 g), 5.0% (5.0 g), and 7.5% (7.5 g) of dry BC (10 g). Each group was dispersed in dH_2O (200 mL) in the presence of an ultrasonic wave (400 W, 20 kHz) generated from a sonicator (Lawson Scientific UP-400S, China) for 25 min. The suspension was stirred at 300 rpm for 2 hours, then BC was added to this suspension and sonicated for an hour. The resulting suspension was then poured into a mold and dried in an oven at 60°C for 24 hours. Once dried, the membranes were saved in a plastic clip and stored in a dry box.

5. Morphology Analysis

The membrane morphology was observed under a Scanning electron microscope (SEM, FEI Inspect-S50, Japan), at 15.0 kV. Before being observed, membrane was coated using gold with a thickness of about 10 nm using a film coater (Emitech-model, England) to improve the membrane conductivity and get a better image of membrane surface.

6. Brunauer-Emmett-Teller (BET) Test

BET (Micromeritics, USA) test with nitrogen as the adsorbate medium was conducted to measure the porosity and specific surface area of composite membranes. Before BET analysis, degassing of membranes was applied to remove any adsorbed gases at 105°C, 4 h.

III. Results and Discussion

1. Surface Morphology Analysis

The result of incorporation of ZnO nanopowder into BC on the membrane morphology is depicted in Figure 1. Figure 1A, control samples, indicates a rough and many voids among fibrous BC. The addition of ZnO nanopowder 2.5% causes the surface of BC membrane to become smoother (Figure 1B) because an amount of ZnO nanopowder interacts with BC internal structure. The higher concentration of ZnO nanopowder (5.0%) exhibits a small agglomeration of ZnO nanopowder on the surface, causing rougher morphology (Figure 1C) due to ZnO nanopowder tend to adhere to adjacent particles [25]. The highest content of ZnO nanopowder (7.5%) leads to a surface fracture and fibrillated cellulose in BC composite

membrane (Figure 1D). ZnO nanopowder was agglomerated on the surface, it is also blended with BC within the membrane, leading to increased ZnO nanopowder agglomeration in the membrane. While a higher amount of ZnO nanopowder interacts effectively with cellulose through hydrogen bonds [26], this strong interaction affects the membrane's morphology.

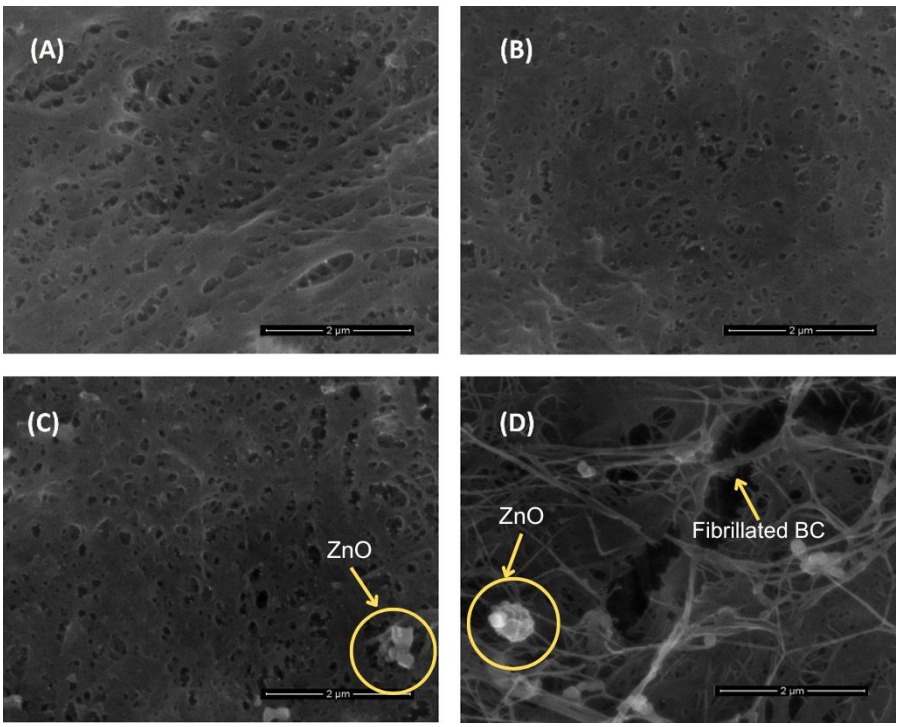

Fig. 1. Surface morphology of BC membrane with ZnO nanopowder reinforcement

2. Brunauer-Emmett-Teller Analysis

The BET surface area plots provide a quantitative assessment of the adsorption characteristics of bacterial cellulose (BC) membranes with varying ZnO nanopowder concentrations (Figure 2). By analyzing the slope and intercept of the linear regions, the monolayer adsorption capacity and the specific surface area of the membranes can be determined, reflecting the impact of ZnO nanopowder reinforcement on surface properties.

Figure 2(A) represents the BET analysis for the unmodified BC membrane, which serves as the control. The specific surface area is 36.9605 m^2/g (Table 1), reflecting the inherent microporous structure of bacterial cellulose. This high surface area arises from the natural, interconnected network of nanofibers in bacterial cellulose, which provides a large number of pores and surface sites for adsorption. The absence of ZnO nanopowder ensures that the porous structure remains uninterrupted, maximizing the accessible surface area. This intrinsic nanofiber structure contributes to the membrane's high surface-to-volume ratio, making it an effective material for adsorption-based applications.

In Figure 2(B), the addition of 2.5% ZnO nanopowder results in a significant reduction in specific surface area to 2.9168 m^2/g (Table 1). This decrease suggests that the initial incorporation of ZnO nanopowder leads to partial pore blockage within the BC matrix, reducing the effective surface area available for adsorption. The nanopowder may fill or obstruct the natural pores, altering the original porous structure of the BC membrane. While

ZnO nanopowder introduces new functional properties, such as antibacterial activity, its presence compromises the inherent porosity of the membrane at this concentration.

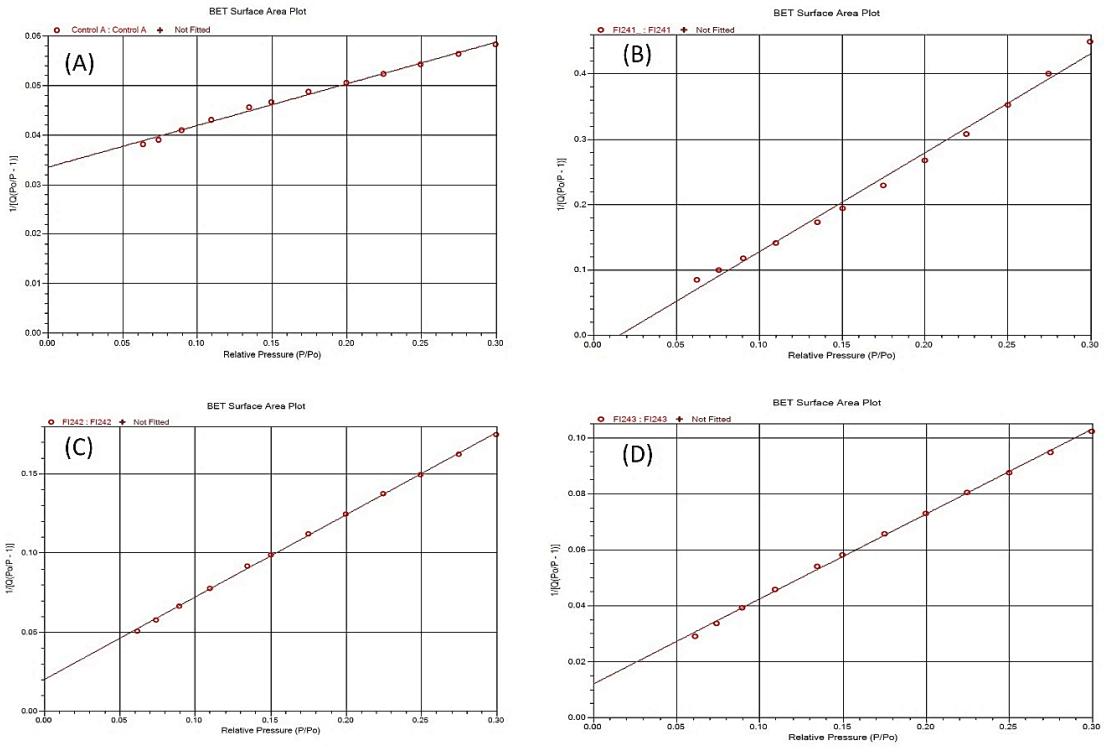

Fig. 2. BET surface area plot

Table 1. Specific Surface Area of ZnO nanopowder added BC

Sample	ZnO Concentration (%)	Specific Surface Area (m^2/g)
(A)	0 (Control)	36.9605
(B)	2.5	2.9168
(C)	5	8.0436
(D)	7.5	13.7783

Figure (C) shows the BET plot for BC with 5% ZnO nanopowder, where the specific surface area increases to 8.0436 m^2/g (Table 1). This increase indicates that the ZnO nanopowder, at this concentration, enhances the structural complexity and surface properties of the membrane. The additional ZnO nanopowder may contribute its surface area and introduce new adsorption sites, partially compensating for the loss of porosity caused by pore obstruction at lower concentrations.

At 7.5% ZnO nanopowder loading, as shown in Figure (D), the specific surface area further increases to 13.7783 m^2/g (Table 1), demonstrating the progressive enhancement of surface properties with higher ZnO nanopowder concentrations. The incorporation of a higher amount of ZnO nanopowder appears to reinforce the composite structure, creating more accessible surface sites. However, the increase between 5% and 7.5% is less pronounced compared to the initial increase, suggesting a gradual stabilization of the surface area improvement.

The BET analysis highlights the complex interaction between ZnO nanopowder and the BC matrix. The control membrane exhibits the highest surface area (36.9605 m^2/g) due to its uninterrupted porous network. The introduction of ZnO nanopowder at 2.5% significantly reduces the surface area to 2.9168 m^2/g, likely due to nanopowder-induced pore obstruction. Increasing the ZnO nanopowder content to 5% and 7.5% increased specific surface area by 8.0436 m^2/g and 13.7783 m^2/g, respectively, which improves porosity and creates more adsorption sites.

Figure 3 depicts the BJH (Barrett–Joyner–Halenda) desorption and adsorption pore volume distribution. Figure 3(A) represents the BJH desorption pore volume distribution of BC membrane without the addition of ZnO nanopowder. It exhibits a dominant peak in the pore diameter range of approximately 5–10 nm, indicating a well-defined mesoporous structure. The control membrane has the highest pore volume compared to the composite membrane, with a specific surface area of 36.9605 m^2/g as determined from the BET analysis. This structure indicates a material suitable for high adsorption capacity, primarily due to the abundance of accessible mesopores.

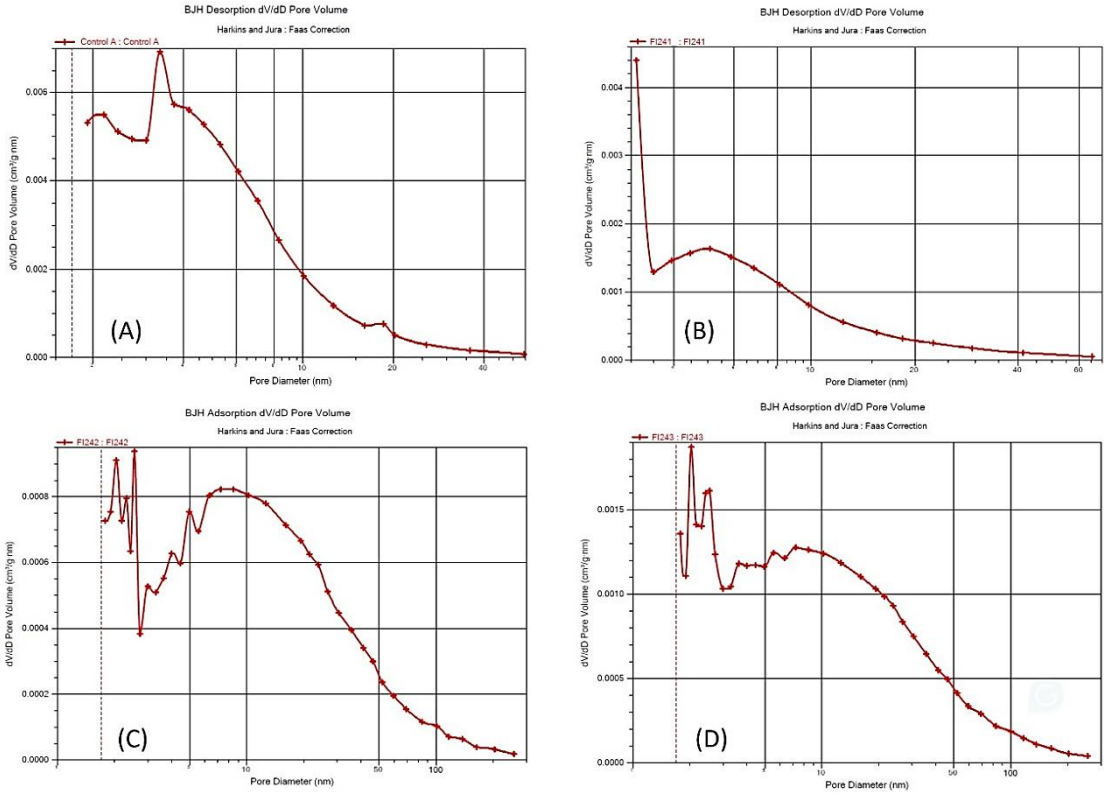

Fig. 3. Barrett–Joyner–Halenda desorption and adsorption pore volume distribution

Figure 3(B) depicts the BJH desorption pore volume distribution for the BC membrane with 2.5% ZnO nanopowder incorporation. The graph demonstrates a significant reduction in the pore volume compared to the control, with the most prominent pores being smaller and less pronounced. The mesoporous structure becomes less distinct, with a shift towards smaller pore diameters. This observation suggests that the incorporation of ZnO nanopowder into the BC membrane reduces the overall porosity, likely due to ZnO nanopowder partially filling the pores or embedding within the BC matrix, thereby blocking some of smaller pores.

Figure 3(C) shows the BJH adsorption pore volume distribution for the BC membrane with 5% ZnO nanopowder. The distribution reflects a slight recovery in pore volume compared to the 2.5% ZnO sample, with a broader pore size distribution extending beyond 10 nm. This indicates that the additional ZnO nanopowder incorporation does not completely block the pores but rather creates a mixed structure of small and intermediate pores. The pore volume trend aligns with the increase in specific surface area (8.0436 m^2/g) observed for this sample.

Figure 3(D) illustrates the BJH adsorption pore volume distribution for the BC membrane with 7.5% ZnO nanopowder. A broad and somewhat irregular distribution of pore diameters is evident, with peaks shifting towards larger diameters (up to 20 nm). The pore volume increases compared to the 5% ZnO nanopowder sample, correlating with the specific surface area of 13.7783 m^2/g. At this concentration, the ZnO nanopowder may aggregate or rearrange within the BC matrix, resulting in the formation of additional voids or larger interconnected pores. This increase in pore volume and diameter is attributed to the ability of ZnO nanopowder to create structural disruptions in the BC matrix, preventing dense packing and allowing larger pores to form.

The control BC membrane exhibits the highest pore volume and well-defined mesoporosity, which are diminished upon the initial addition of ZnO nanopowder due to partial pore blocking. However, at higher ZnO nanopowder concentrations (5% and 7.5%), the structural disruption caused by ZnO nanopowder within the BC matrix generates new voids and larger pores. Various studies have shown that adding ZnO nanopowder during membrane formation generally increases the membrane's pore size [27],[28]. While the average pore sizes in molecular sieve membranes are greater than 0.3-0.5 nm, they remain smaller than the pore sizes of 10 nm-1 μm typically found in polymeric membranes used for membrane distillation systems [29].

Sharp peaks (as seen in the control sample) indicate a uniform pore structure, while broad peaks (as in 5% and 7.5% ZnO nanopowder samples) reflect a more heterogeneous pore size distribution. Peak height reflects the relative pore volume at a given size, with higher peaks indicating a greater abundance of pores in that size range. Shifts in peaks (to smaller or larger diameters) indicate changes in pore size distribution, which in this case are due to ZnO nanopowder incorporation affecting the BC matrix. This behavior may result from ZnO nanopowder aggregation or the introduction of nanopowder–matrix interactions that expand the overall pore structure. The BJH analysis from the BET results provides insight into the structural transformations of BC membranes with ZnO nanopowder addition, which influences membrane adsorption and filtration characteristics.

From the result, higher ZnO loading may promote the formation of more porous or fibrillated structures, potentially due to changes in the BC matrix or nanoparticle distribution. From an application perspective, variations in surface area play a critical role [30]. Membranes with greater surface area offer more active sites for interaction with bacteria and contaminants, making them particularly advantageous for use in water purification and antimicrobial technologies.

4. Conclusion

This study has successfully shown the effect of ZnO nanopowder addition to BC membranes on porosity, pore volume, and surface morphology. The BET analysis on gas desorption and adsorption of the membrane indicates structural transformations of BC matrix with increasing ZnO nanopowder content. The BC membrane had the highest specific

surface area of 36.9605 m^2/g. After adding 2.5% ZnO nanopowder, the pore volume was reduced, and a shift to smaller pore diameters was observed. Interestingly, as the ZnO nanopowder content increased to 5% and 7.5%, pore sizes had a broader distribution and an increase in pore volume. With 7.5% ZnO nanopowder, membrane structure heterogeneity became more evident, characterized by increasingly larger pores reaching up to 20 nm and in specific surface area of 13.7783 m^2/g. Such modifications have critical implications for enhancing the adsorption, filtration, and overall performance of BC-based materials in various applications. Future work can explore the functional implications of these membrane applications, such as water purification, biomedical devices, and catalysis.

Acknowledgment

Sincere appreciation is extended to LPPM-UM and DPPM Dikti for their support through the Fundamental Research grant with contract no. 11.6.81/UN32.14.1/LT/2024.

References

[1] Badan Pusat Statistik (BPS), "Lampung Produsen Nanas Terbesar Di Indonesia Tahun 2023," PPID Provinsi Lampung, Published January 5, 2024, Available: https://ppid.lampungprov.go.id/detail-post/Lampung-Produsen-Nanas-Terbesar-Di-Indonesia-Tahun-2023#

[2] Pusat Data dan Sistem Informasi Pertanian, *Outlook Komoditas Hortikultura: Nanas*, Ministry of Agriculture of Indonesia, Jakarta, 2023.

[3] P.K. Sarangi, T.A. Singh, N.J. Singh, K.P. Shadangi, R.K. Srivastava, A.K. Singh *et al*., "Sustainable utilization of pineapple wastes for production of bioenergy, biochemicals and value-added products: A review," *Bioresour Technol*, vol. 351, p. 127085, 2022, doi: h10.1016/j.biortech.2022.127085.

[4] S.K. Bhatia, S. Mehariya, R.K. Bhatia, M. Kumar, A. Pugazhendhi, M.K. Awasthi *et al*., "Wastewater based microalgal biorefinery for bioenergy production: Progress and challenges," *Science of the Total Environment*, vol. 751, p. 141599, 2021, doi: 10.1016/j.scitotenv.2020.141599.

[5] H. Suryanto, F. Kurniawan, D. Syukri, J.S. Binoj, P.D. Hari, and U. Yanuhar, "Properties of bacterial cellulose acetate nanocomposite with TiO_2 nanoparticle and graphene reinforcement," *Int J Biol Macromol*, vol. 235, p. 123705, 2023, doi: 10.1016/j.ijbiomac.2023.123705.

[6] I. Ryłko-Polak, W. Komala, and A. Białowiec, "The reuse of biomass and industrial waste in biocomposite construction materials for decreasing natural resource use and mitigating the environmental impact of the construction industry: A review," *Materials*, vol. 15, no. 12, p. 4078, 2022, doi: 10.3390/ma15124078.

[7] J. Huang, X. Ma, A. Dufresne, and Y. Guang, Nanocellulose: From fundamentals to advanced materials, in: J. Huang, A. Dufresne, N. Lin, "Nanocellulose: From fundamentals to advanced materials," *Wiley-VCH*, *(Germany),* pp. 1–486, 2019, doi: 10.1002/9783527807437.

[8] L. Pessoni, S. Lacombe, L. Billon, R. Brown, and M. Save, "Photoactive, porous honeycomb films prepared from rose bengal-grafted polystyrene," *Langmuir*, vol. 29, no. 32, pp. 10264–10271, 2013, doi: 10.1021/la402079z.

[9] K. Pourzare, Y. Mansourpanah, and S. Farhadi, "Advanced nanocomposite membranes for fuel cell applications: A comprehensive review," *Biofuel Research Journal*, vol. 3, pp. 496–513, 2016, doi: 10.18331/BRJ2016.3.4.4.

[10] L. Zheng, S. Li, J. Luo, and X. Wang, "Latest advances on bacterial cellulose-based

antibacterial materials as wound dressings," *Front Bioeng Biotechnol*, vol. 8, p. 593768, 2020, doi: 10.3389/fbioe.2020.593768.

[11] B.K. Tripathi and P. Pandey, "Breath figure templating for fabrication of polysulfone microporous membranes with highly ordered monodispersed porosity," *J Memb Sci*, vol. 471, pp. 201–210, 2014, doi: 10.1016/j.memsci.2014.08.004.

[12] L.A.N. El-Din, A. El-Gendi, N. Ismail, K.A. Abed, and A.I. Ahmed, "Evaluation of cellulose acetate membrane with carbon nanotubes additives," *Journal of Industrial and Engineering Chemistry*, vol. 26, pp. 259–264, 2015, doi: 10.1016/j.jiec.2014.11.037.

[13] M. Safarpour, A. Khataee, and V. Vatanpour, "Thin film nanocomposite reverse osmosis membrane modified by reduced graphene oxide/TiO_2 with improved desalination performance," *J. Memb. Sci.*, vol. 489, pp. 43–54, 2015, doi: 10.1016/j.memsci.2015.04.010.

[14] L. Yu and A.L. Skov, "ZnO as a cheap and effective filler for high breakdown strength elastomers," *RSC Adv*, vol. 7, pp. 45784–45791, 2017, doi: 10.1039/C7RA09479E.

[15] D.K. Sharma, S. Shukla, K.K. Sharma, and V. Kumar, "A review on ZnO: Fundamental properties and applications," *Materials Today Proc.*, vol. 49, pp. 3028–3035, 2022, doi: 10.1016/j.matpr.2020.10.238.

[16] S. V Gudkov, D.E. Burmistrov, D.A. Serov, M.B. Rebezov, A.A. Semenova, and A.B. Lisitsyn, "A mini review of antibacterial properties of ZnO nanoparticles," *Frontiers in Physics*, vol. 9, 2021, doi: 10.3389/fphy.2021.641481

[17] R. Kumar, A. Umar, G. Kumar, and H.S. Nalwa, "Antimicrobial properties of ZnO nanomaterials: A review," *Ceram. Int.*, vol. 43, pp. 3940–3961, 2017, doi: 10.1016/j.ceramint.2016.12.062.

[18] H. Hamrayev and K. Shameli, "Biopolymer-based green synthesis of zinc oxide (ZnO) nanoparticles," *IOP Conf. Ser. Mater. Sci. Eng.*, vol. 1051, p. 012088, 2021, doi: 10.1088/1757-899x/1051/1/012088.

[19] B.L. Guo, P. Han, L.C. Guo, Y.Q. Cao, A.D. Li, J.Z. Kong *et al*., "The antibacterial activity of Ta-doped ZnO nanoparticles," *Nanoscale Res. Lett.*, vol. 10, no. 336, 2015, doi: 10.1186/s11671-015-1047-4.

[20] J. Supramaniam, D.Y.S. Low, S.K. Wong, L.T.H. Tan, B.F. Leo, B.H. Goh *et al*., "Facile synthesis and characterization of palm CNF-ZnO nanocomposites with antibacterial and reinforcing properties," *Int. J. Mol. Sci.*, vol. 22, no. 11, p. 5781, 2021, doi: 10.3390/ijms22115781.

[21] M. Khikani, G.O. Isopencu, I.M. Deleanu, S.I. Jinga, and C. Busuioc, "Green Synthesis of Nanoparticle-Loaded Bacterial Cellulose Membranes with Antibacterial Properties," *J. Compos. Sci.*, vol. 8, no. 11, p. 475, 2024, doi: 10.3390/jcs8110475.

[22] F. Wahid, Y.-X. Duan, X.-H. Hu, L.-Q. Chu, S.-R. Jia, J.-D. Cui, and C. Zhong, "A facile construction of bacterial cellulose/ZnO nanocomposite films and their photocatalytic and antibacterial properties," *Int. J. Biol. Macromol.*, vol. 132, pp. 692–700, 2019, doi: 10.1016/j.ijbiomac.2019.03.240.

[23] H.B. Sharma, K.R. Vanapalli, B. Samal, V.R.S. Cheela, B.K. Dubey, and J. Bhattacharya, "Circular economy approach in solid waste management system to achieve UN-SDGs: Solutions for post-COVID recovery," *Science of The Total Environment*, vol. 800, p. 149605, 2021, doi: 10.1016/j.scitotenv.2021.149605.

[24] S.A. Sardjono, H. Suryanto, Aminnudin, and M. Muhajir, "Crystallinity and morphology of the bacterial nanocellulose membrane extracted from pineapple peel waste using high-pressure homogenizer," *AIP. Conf. Proc.*, vol. 2120, no. 1, 2019,

doi: 10.1063/1.5115753.

[25] R.S. Dubey and S. Singh, "Investigation of structural and optical properties of pure and chromium doped TiO2 nanoparticles prepared by solvothermal method," *Results Phys.*, vol. 7, pp.1283–1288, 2017, doi: 10.1016/j.rinp.2017.03.014.

[26] X. Li, H. Li, X. Wang, D. Xu, T. You, Y. Wu, and F. Xu, "Facile in situ fabrication of ZnO-embedded cellulose nanocomposite films with antibacterial properties and enhanced mechanical strength via hydrogen bonding interactions," *Int. J. Biol. Macromol.*, vol. 183, pp. 760–771, 2021, doi: 10.1016/j.ijbiomac.2021.04.175.

[27] T. Istirokhatun, U. Yuni, P. Andarani, and H. Susanto, "Do ZnO and Al_2O_3 nanoparticles improve the anti-bacterial properties of cellulose acetate-chitosan membrane?," *MATEC Web Conf*, vol. 156, p. 08009, 2018, doi: 10.1051/matecconf/201815608009.

[28] A.M. Asiri, F. Petrosino, V. Pugliese, S.B. Khan, K.A. Alamry, S.Y. Alfifi *et al*., "Synthesis and characterization of blended cellulose acetate membranes," *Polymers (Basel)*, vol. 14, no. 1, p. 4, 2022, doi: 10.3390/polym14010004.

[29] L. Camacho, L. Dumée, J. Zhang, J. Li, M. Duke, J. Gomez, and S. Gray, "Advances in membrane distillation for water desalination and purification applications," *Water (Basel)*, vol. 5, no. 1, pp. 94–196, 2013, doi: 10.3390/w5010094.

[30] B. Chamam, R.B. Dassi, J. Abderraouf, J.P. Mericq, C. Faur, I. Trabelsi *et al*., "Incorporation of Ag-ZnO nanoparticles into PVDF membrane formulation to enhance dye retention, permeability, and antibacterial properties," *Polymers (Basel)*, vol. 17, no. 9, p. 1269, 2025, doi: 10.3390/polym17091269.